

## Transformed Eliassen Balanced Vortex Model

WAYNE H. SCHUBERT

*Department of Atmospheric Sciences, Colorado State University, Fort Collins, CO 80523*

JAMES J. HACK

*IBM Thomas J. Watson Research Center, Yorktown Heights, NY 10598*

(Manuscript received 13 November 1982, in final form 10 February 1983)

### ABSTRACT

We consider the axisymmetric balanced flow occurring in a thermally forced vortex in which the frictional inflow is confined to a thin boundary layer. Above the boundary layer the absolute angular momentum  $\frac{1}{2}fR^2 = rv + \frac{1}{2}fr^2$  is conserved. We refer to  $R$  as the potential radius, i.e., the radius to which a particle must be moved (conserving absolute angular momentum) in order to change its tangential component  $v$  to zero. Using  $R$  as one of the dependent variables we review the equations of the Eliassen balanced vortex model.

We next reverse the roles of the actual radius  $r$  and the potential radius  $R$ , i.e., we treat  $R$  as an independent variable and  $r$  as a dependent variable. Introducing transformed components ( $u^*$ ,  $w^*$ ) of the transverse circulation we obtain the transformed Eliassen balanced vortex equations, which differ from the original equations in the following respects: 1) the radial coordinate is  $R$  which results in a stretching of positive relative vorticity regions and a shrinking of negative relative vorticity regions; 2) the thermodynamic equation contains only the transverse circulation component  $w^*$ , the coefficient of which is the potential vorticity  $q$ ; 3) the equation for  $r$  contains only the transverse circulation component  $u^*$ ; 4) the transverse circulation equation contains only two vortex structure functions, the potential vorticity  $q$  and the inertial stability  $s$ , where  $\rho q = (\zeta/f)(g/\theta_0)(\partial\theta/\partial Z)$  and  $\rho s = f^2 R^4/r^4$ .

The form of the transverse circulation equation leads naturally to a generalized Rossby radius proportional to  $(q/s)^{1/2}$ . A typical distribution of  $(q/s)^{1/2}$  is calculated using the composite tropical cyclone data of Gray. The fundamental dynamical role of  $(q/s)^{1/2}$  is then illustrated with a simple analytical example.

### 1. Introduction

The equations which describe the slow, quasi-balanced evolution of a thermally or frictionally controlled axisymmetric vortex were introduced by Eliassen (1952). Simplification of these equations and introduction of parameterized cumulus convection formed the basis of the CISK theories of Ooyama (1964) and Charney and Eliassen (1964). Eliassen's balanced vortex equations were also the basis of several nonlinear, numerical, tropical cyclone models (e.g., Ooyama, 1969a; Sundqvist, 1970). In the past decade, simulation and prediction efforts have shifted toward the use of the primitive equations in two and three dimensions. However, Eliassen's model continues to help in understanding the development of tropical vortex flows (e.g., Shapiro and Willoughby, 1982; Schubert and Hack, 1982) and in interpretation of research aircraft data on cycles of intensification and variations in eye diameter (Willoughby *et al.*, 1982).

The purpose of the present work is to derive a new and somewhat simpler form of Eliassen's balanced vortex model. We first review (Section 2) Eliassen's model in a form which uses the potential radius  $R$

(where  $\frac{1}{2}fR^2 = rv + \frac{1}{2}fr^2$ ) as one of the dependent variables and the actual radius  $r$  as one of the independent variables. In Section 3 we reverse the roles of  $R$  and  $r$ , obtaining the transformed Eliassen balanced vortex model. Certain aspects of the transformed model are similar to those of Hoskins' semi-geostrophic equations (see Hoskins, 1975; Hoskins and Draghici, 1977), e.g., the stretching of high vorticity regions and the role of potential vorticity as a static stability. However, as far as axisymmetric flows are concerned, the transformed Eliassen equations are more general than the semi-geostrophic equations since the Eliassen equations are valid for the highly curved flows occurring in tropical cyclones. In Section 4 we interpret some of the composite tropical cyclone data of Gray in terms of the transformed equations. The simple form of the transverse circulation equation which occurs in the transformed model leads naturally to a new definition of the Rossby radius. In Section 5 we present a simple analytical argument which illustrates the important dynamical role played by this Rossby radius in the development of a tropical cyclone.

## 2. Eliassen balanced vortex model

We consider the axi-symmetric, balanced flow occurring in a thermally forced vortex on an  $f$ -plane. We assume that frictional stresses are confined to a thin boundary layer and thus that the flow above the boundary layer is frictionless. The effects of friction on the free atmosphere are then felt through a condition on the vertical velocity at the top of the boundary layer. In the following we consider separately the governing equations for the motion in the free atmosphere and the motion in the boundary layer.

### a. Motion in the free atmosphere

Using the Hoskins and Bretherton (1972) pseudo-height coordinate

$$z = \left[ 1 - \left( \frac{p}{p_0} \right)^\kappa \right] \frac{c_p \theta_0}{g},$$

the gradient wind balance, conservation of absolute angular momentum, hydrostatic balance, mass continuity and the thermodynamic equations can be written as

$$\frac{1}{4} f^2 (R^4 - r^4) = r^3 \frac{\partial \phi}{\partial r}, \quad (2.1)$$

$$\frac{DR}{Dt} = 0, \quad (2.2)$$

$$\frac{\partial \phi}{\partial z} = \frac{g}{\theta_0} \theta, \quad (2.3)$$

$$\frac{\partial ru}{r \partial r} + \frac{\partial \rho w}{\rho \partial z} = 0, \quad (2.4)$$

$$c_p \frac{D \ln \theta}{Dt} = \frac{Q}{T}, \quad (2.5)$$

where  $u$ ,  $v$ ,  $w$  are the radial, tangential and vertical components of velocity,  $\frac{1}{2} f R^2 = rv + \frac{1}{2} f r^2$  is the absolute angular momentum per unit mass,  $\rho = \rho_0 [1 - (gz/c_p \theta_0)]^{(1-\kappa)/\kappa}$  is the pseudo-density (a known function of  $z$ ),  $T$  is the temperature,  $\phi$  the geopotential,  $D/Dt = \partial/\partial t + u\partial/\partial r + w\partial/\partial z$ ,  $Q$  is assumed to be a specified function of space and time, and subscript zero denotes a "top of the boundary layer" value. The potential radius  $R$  is the radius to which a particle must be moved (conserving absolute angular momentum) in order to change its relative angular momentum to zero. We assume that  $R$  is real and positive.

### b. Motion in the boundary layer

Following Ogura (1964) and Ooyama (1969a) we shall assume that in the boundary layer the pressure gradient force does not vary with height and gradient

balance exists.<sup>1</sup> In addition, we assume the layer is so shallow that we can neglect the variation of pseudo-density and the local time derivative in the tangential wind equation. With these assumptions we can write the tangential wind and continuity equations as

$$\left( f + \frac{\partial r v_0}{r \partial r} \right) hu + c_D |v_0| v_0 = 0, \quad (2.6)$$

$$h \frac{\partial ru}{r \partial r} + w_0 = 0, \quad (2.7)$$

where  $u$  is the radial component of velocity in the boundary layer,  $v_0$  and  $w_0$  are the tangential and vertical components of velocity at the top of the boundary layer,  $h$  the depth of the boundary layer and  $c_D$  the drag coefficient. Eliminating  $hu$  between (2.6) and (2.7) yields

$$w_0 = \frac{\partial}{\partial r} \left[ \frac{f}{\xi_0} c_D |v_0|^{1/2} (R_0^2 - r^2) \right], \quad (2.8)$$

where  $\xi_0$  is the vertical component of absolute vorticity at the top of the boundary layer. Eq. (2.8) provides the necessary lower boundary condition for the system (2.1)–(2.5).

### c. Pseudo-conservation relations

The Eliassen balanced vortex model (2.1)–(2.5) is a filtered intermediate model (McWilliams and Gent, 1980). It is filtered in the sense that gravity-inertia waves and the transient aspects of gradient wind adjustment are not included. It is intermediate in the sense that its accuracy lies somewhere above the quasi-geostrophic model, but below the primitive equation model. Because of the inclusion of curvature effects the Eliassen balanced vortex model also lies somewhat above the axisymmetric version of the geostrophic momentum approximation in accuracy. Just as the geostrophic momentum approximation is capable of describing many of the nonlinear aspects of fronts and jets, the Eliassen balanced vortex model is apparently capable of describing many of the nonlinear aspects of tropical cyclone development. As pointed out by Hoskins (1975), the equations with the geostrophic momentum approximation preserve the forms of the pseudo-conservation relations for potential temperature, vector vorticity, Ertel's potential vorticity, and energy. A similar result holds for

<sup>1</sup> Both Ogura (1964) and Ooyama (1969a) acknowledge that the assumption of gradient wind balance in the boundary layer is crude. Ooyama (1969b) has shown that more realistic tropical cyclone simulations can be achieved by using a hybrid model (gradient balance above the boundary layer and quasi-steady-state primitive equations in the boundary layer). A similar conclusion (but with a somewhat different hybrid model) was reached by Peng and Kuo (1975).

the Eliassen balanced vortex equations, in which case the pseudo-conservation relations take the forms:

1) POTENTIAL TEMPERATURE EQUATION

$$\frac{D\theta}{Dt} = Q, \quad \text{where} \quad Q = \left(1 - \frac{gz}{c_p\theta_0}\right)^{-1} \frac{Q}{c_p}$$

2) VECTOR VORTICITY EQUATION

$$\frac{D\zeta}{Dt} = (\zeta \cdot \nabla)\mathbf{u} + \zeta w \frac{\partial \rho}{\rho \partial z},$$

where

$$\zeta = \left(-\frac{\partial v}{\partial z}, f + \frac{\partial rv}{r\partial r}\right) = f \left(-\frac{\partial}{r\partial z} \left(\frac{R^2}{2}\right), \frac{\partial}{r\partial r} \left(\frac{R^2}{2}\right)\right)$$

and

$$\mathbf{u} = (u, w).$$

3) ERTEL POTENTIAL VORTICITY EQUATION

$$\frac{Dq}{Dt} = \frac{g}{f\theta_0\rho} \zeta \cdot \nabla Q,$$

where

$$q = \frac{g}{f\theta_0\rho} \zeta \cdot \nabla \theta.$$

4) ENERGY EQUATION

$$\rho \frac{D}{Dt} (K + P) + \nabla \cdot (\rho \mathbf{u} \phi) = -\frac{g}{\theta_0} \rho z Q,$$

where

$$K = \frac{1}{2}v^2 \quad \text{and} \quad P = -\frac{g}{\theta_0} z\theta.$$

The only difference between the above relations and those obtained from the primitive equations is the neglect of  $\frac{1}{2}u^2$  in  $K$  and the use of the gradient wind in the determination of  $\zeta$ ,  $q$  and  $K$ .

d. Transverse circulation equation

Although the set (2.1)–(2.5) is closed in the unknowns,  $u$ ,  $R$ ,  $w$ ,  $\theta$  and  $\phi$ , it is not a convenient set for computation. A computationally convenient set is one in which either of the prognostic equations (2.2) or (2.5) is replaced by a diagnostic equation for the transverse circulation ( $\rho u$ ,  $\rho w$ ), which, because of the continuity equation, can be expressed in terms of the single streamfunction variable  $\psi$  as

$$(\rho u, \rho w) = \left(-\frac{\partial \psi}{\partial z}, \frac{\partial r\psi}{r\partial r}\right). \quad (2.9)$$

The diagnostic equation for  $\psi$  is derived by combining (2.1) and (2.3) to obtain

$$f^2 \frac{R^3}{r^3} \frac{\partial R}{\partial z} = \frac{g}{\theta_0} \frac{\partial \theta}{\partial r}, \quad (2.10)$$

and using this “thermal wind equation” to eliminate local time derivatives between (2.2) and (2.5). The result is

$$\frac{\partial}{\partial r} \left( A \frac{\partial r\psi}{r\partial r} + B \frac{\partial \psi}{\partial z} \right) + \frac{\partial}{\partial z} \left( B \frac{\partial r\psi}{r\partial r} + C \frac{\partial \psi}{\partial z} \right) = \frac{g}{\theta_0} \frac{\partial Q}{\partial r}, \quad (2.11a)$$

where

$$\rho A = \frac{g}{\theta_0} \frac{\partial \theta}{\partial z} \quad (\text{static stability}) \quad (2.11b)$$

$$\rho B = -\frac{g}{\theta_0} \frac{\partial \theta}{\partial r} = -f^2 \frac{R^3}{r^3} \frac{\partial R}{\partial z} \quad (\text{baroclinity}) \quad (2.11c)$$

$$\rho C = f^2 \frac{R^3}{r^3} \frac{\partial R}{\partial r} \quad (\text{inertial stability}). \quad (2.11d)$$

The boundary conditions for (2.11a) are

$$\left. \begin{aligned} \psi(0, z) &= \psi(r, z_T) = 0 \\ r\psi &\rightarrow 0 \quad \text{as} \quad r \rightarrow \infty \\ r\psi_0 &= \frac{f}{\xi_0} \rho_0 c_D |v_0| \frac{1}{2} (R_0^2 - r^2) \end{aligned} \right\}, \quad (2.11e)$$

the last of which is easily derived from (2.8) and (2.9).

e. Summary of the balanced vortex model

We can now collect the results (2.10), (2.11), (2.9), (2.5) and (2.2) applied at  $z = 0$  to obtain the system of equations given on the left side of Table 1. A single step in the numerical integration of (2.12)–(2.19) proceeds as follows. Knowing  $\theta(r, z)$  and  $R_0(r)$  from an initial condition or a previous time step we can solve (2.12) for  $R(r, z)$ . After using (2.13)–(2.15) to compute  $A$ ,  $B$  and  $C$ , we solve (2.16) for  $\psi(r, z)$ . After computing  $u$  and  $w$  from (2.17), we predict new values of  $\theta(r, z)$  and  $R_0(r)$  from (2.18) and (2.19).

3. Coordinate transformation

We now wish to reverse the roles of  $r$  and  $R$ , *i.e.*, we now consider  $R$  to be the independent variable and  $r$  the dependent variable. For convenience we also introduce  $T = t$  and  $Z = z$ , but we note that  $\partial/\partial T \neq \partial/\partial t$  and  $\partial/\partial Z \neq \partial/\partial z$  since  $\partial/\partial T$  and  $\partial/\partial Z$  indicate that  $R$  is held fixed. The transformation used here is an adaptation to the Eliassen balanced vortex model of transformations which have proved useful in other problems, primarily frontogenesis. The advantages of “absolute momentum coordinates” or “geostrophic coordinates” were pointed out in the two dimensional frontal studies of Eliassen (1962) and Hoskins and Bretherton (1972). The generaliza-

TABLE 1. Comparison of the governing equations for the original model and the transformed model.

Eliassen model	Transformed Eliassen model
$f^2 \frac{R^3}{r^3} \frac{\partial R}{\partial z} = \frac{g}{\theta_0} \frac{\partial \theta}{\partial r}$ (2.12)	$-f^2 \frac{R^3}{r^3} \frac{\partial r}{\partial Z} = \frac{g}{\theta_0} \frac{\partial \theta}{\partial R}$ (3.23)
$\rho A = \frac{g}{\theta_0} \frac{\partial \theta}{\partial z}$ (2.13)	$\frac{f}{\zeta} = \frac{\partial}{R \partial R} \left( \frac{r^2}{2} \right)$ (3.24)
$\rho B = -\frac{g}{\theta_0} \frac{\partial \theta}{\partial r} = -f^2 \frac{R^3}{r^3} \frac{\partial R}{\partial z}$ (2.14)	$\rho q = \frac{\zeta}{f} \frac{g}{\theta_0} \frac{\partial \theta}{\partial Z}$ (3.25)
$\rho C = f^2 \frac{R^3}{r^3} \frac{\partial R}{\partial r}$ (2.15)	$\rho s = f^2 \frac{R^4}{r^4}$ (3.26)
$\left\{ \begin{aligned} &\frac{\partial}{\partial r} \left( A \frac{\partial r \psi}{r \partial r} + B \frac{\partial \psi}{\partial z} \right) + \frac{\partial}{\partial z} \left( B \frac{\partial r \psi}{r \partial r} + C \frac{\partial \psi}{\partial z} \right) = \frac{g}{\theta_0} \frac{\partial Q}{\partial r} \\ &\text{B.C. } \psi(0, z) = \psi(r, z_T) = 0, \quad r\psi \rightarrow 0 \text{ as } r \rightarrow \infty \\ &r\psi(r, 0) = \frac{f}{\zeta_0} \rho_0 C_D  v_0  \frac{1}{2} (R_0^2 - r^2) \end{aligned} \right\}$	$\left\{ \begin{aligned} &\frac{\partial}{\partial R} \left( q \frac{\partial R \psi^*}{R \partial R} \right) + \frac{\partial}{\partial Z} \left( s \frac{\partial \psi^*}{\partial Z} \right) = \frac{g}{\theta_0} \frac{\partial Q}{\partial R} \\ &\text{B.C. } \psi^*(0, Z) = \psi^*(R, Z_T) = 0, \\ &R\psi^* \rightarrow 0 \text{ as } R \rightarrow \infty, \\ &R\psi^*(R, 0) = \frac{f}{\zeta_0} \rho_0 C_D  v_0  \frac{1}{2} (R^2 - r_0^2) \end{aligned} \right\}$
$(\rho u, \rho w) = \left( -\frac{\partial \psi}{\partial z}, \frac{\partial r \psi}{r \partial r} \right)$ (2.17)	$(\rho u^*, \rho w^*) = \left( -\frac{\partial \psi^*}{\partial Z}, \frac{\partial R \psi^*}{R \partial R} \right)$ (3.28)
$\frac{\partial \theta}{\partial t} + \frac{\theta_0}{g} (\rho A w + \rho B u) = Q$ (2.18)	$\frac{\partial \theta}{\partial T} + \frac{\theta_0}{g} \rho q w^* = Q$ (3.29)
$f^2 \frac{R_0^3}{r^3} \frac{\partial R_0}{\partial t} - \rho_0 B_0 w_0 + \rho_0 C_0 u_0 = 0$ (2.19)	$f^2 \frac{R^3}{r_0^3} \frac{\partial r_0}{\partial T} - \rho_0 s_0 u_0^* = 0$ (3.30)

tion to three dimensions has been given by Hoskins (1975) and Hoskins and Draghici (1977). These ideas have also been used for flows on both the *f*-plane and sphere by Shutts and Thorpe (1978) and Shutts (1980), and in an oceanographic context by Gill (1981) in his study of homogeneous intrusions of mass in a rotating, stratified fluid.

To transform to these new coordinates we make use of

$$\frac{\partial}{\partial t} = \frac{\partial}{\partial T} + \frac{\partial R}{\partial t} \frac{\partial}{\partial R}, \tag{3.1}$$

$$\frac{\partial}{\partial r} = \frac{\partial R}{\partial r} \frac{\partial}{\partial R}, \tag{3.2}$$

$$\frac{\partial}{\partial z} = \frac{\partial R}{\partial z} \frac{\partial}{\partial R} + \frac{\partial}{\partial Z}. \tag{3.3}$$

From (3.1)–(3.3) and absolute angular momentum conservation, it is easily shown that

$$\frac{D}{Dt} = \frac{\partial}{\partial T} + w \frac{\partial}{\partial Z}, \tag{3.4}$$

so that radial advection will not appear in the transformed equations. Since the dimensionless vertical component of absolute vorticity  $\zeta f^{-1}$  can be written as  $\partial(\frac{1}{2}R^2/r\partial r)$ , we can write (3.2) as

$$\frac{\partial}{r \partial r} = \frac{\zeta}{f} \frac{\partial}{R \partial R}. \tag{3.5}$$

Eqs. (3.2) and (3.3) can also be combined to obtain

$$\zeta \cdot \nabla = \zeta \frac{\partial}{\partial Z}, \tag{3.6}$$

which allows us to write the potential vorticity in the simpler but exact form

$$q = \frac{g}{f \theta_0 \rho} \zeta \frac{\partial \theta}{\partial Z}, \tag{3.7}$$

where  $\zeta$  is the vertical component of  $\zeta$ .

In analogy with Hoskins and Draghici (1977) we define the new components of the transverse circulation by

$$Ru^* = r \left( u - w \frac{\partial r}{\partial Z} \right), \tag{3.8}$$

$$w^* = \frac{f}{\zeta} w. \tag{3.9}$$

Then, using (3.4), (3.8) and (3.7) the tangential wind equation (2.2) and the thermodynamic equation (2.5) can be written as

$$\frac{\partial}{\partial T} \left( \frac{r^2}{2} \right) - Ru^* = 0, \tag{3.10}$$

$$\frac{\partial \theta}{\partial T} + \frac{\theta_0}{g} q \rho w^* = Q. \tag{3.11}$$

Thus, only the component  $u^*$  contributes to a change in the horizontal area within an angular momentum surface and only the component  $w^*$  contributes to a change in potential temperature on the angular momentum surface.

As in Hoskins' semi-geostrophic theory the transformed continuity equation can be derived from the vertical component of the vorticity equation, which can be written

$$\frac{\partial \zeta}{\partial T} + w \frac{\partial \zeta}{\partial Z} - \zeta \frac{\partial \rho w}{\rho \partial Z} = 0. \tag{3.12}$$

Using (3.9) this becomes

$$\frac{\partial}{\partial T} \left( \frac{f}{\zeta} \right) + \frac{\partial \rho w^*}{\rho \partial Z} = 0. \tag{3.13}$$

Applying (3.5) to  $rv$  we obtain

$$\frac{f}{\zeta} = 1 - \frac{1}{f} \frac{\partial rv}{R \partial R} = \frac{\partial}{R \partial R} \left( \frac{r^2}{2} \right). \tag{3.14}$$

Substituting (3.14) into (3.13) and using (3.10) we obtain the transformed continuity equation

$$\frac{\partial Ru^*}{R \partial R} + \frac{\partial \rho w^*}{\rho \partial Z} = 0, \tag{3.15}$$

which has the same form as (2.4).

Applying (3.3) to  $r^2$  and using (3.14) we obtain

$$-\frac{\zeta}{f} \frac{\partial r^2}{\partial Z} = \frac{\partial R^2}{\partial z}.$$

Using this along with (3.5) we can transform the thermal wind equation<sup>2</sup> (2.10) to

$$-f^2 \frac{R^3}{r^3} \frac{\partial r}{\partial Z} = \frac{g}{\theta_0} \frac{\partial \theta}{\partial R}. \tag{3.16}$$

Since the tendencies of  $r$  and  $\theta$  from (3.10) and (3.11) must be consistent with the thermal wind equation (3.16), a diagnostic equation for the transverse circulation ( $\rho u^*$ ,  $\rho w^*$ ) is implied. This equation is derived by taking the  $Z$  derivative of  $f^2 R^3/r^4$  times (3.10) and the  $R$  derivative of  $g/\theta_0$  times (3.11), and using the fact that

<sup>2</sup> It is also possible to obtain (3.16) by first transforming the gradient wind and hydrostatic equations. For this purpose it is convenient to define  $\Phi = \phi + \frac{1}{2}v^2 = \phi + \frac{1}{2}f^2(R^2 - r^2)r^{-2}$ . Then the transformed gradient wind equation becomes  $\frac{1}{2}f^2R(R^2 - r^2)r^{-2} = \partial\Phi/\partial R$  and the transformed hydrostatic equation  $(g/\theta_0)\theta = \partial\Phi/\partial Z$ , from which (3.16) immediately follows. When  $R/r \approx 1$  the above relation for  $\Phi$  can be approximated by  $\Phi \approx \phi + \frac{1}{2}f^2(R - r)^2$ , which is the form taken in semi-geostrophic theory.

$$\frac{\partial}{\partial Z} \left( \frac{\partial r}{r^3 \partial T} \right) = \frac{\partial}{\partial T} \left( \frac{\partial r}{r^3 \partial Z} \right),$$

to obtain

$$\frac{\partial}{\partial T} \left( -f^2 \frac{R^3}{r^3} \frac{\partial r}{\partial Z} \right) + \frac{\partial}{\partial Z} (s \rho u^*) = 0, \tag{3.17}$$

$$\frac{\partial}{\partial T} \left( \frac{g}{\theta_0} \frac{\partial \theta}{\partial R} \right) + \frac{\partial}{\partial R} (q \rho w^*) = \frac{g}{\theta_0} \frac{\partial Q}{\partial R}, \tag{3.18}$$

where the inertial stability  $s$  is given by

$$\rho s = f^2 \frac{R^4}{r^4}. \tag{3.19}$$

Subtracting (3.17) from (3.18) and using (3.16) yields

$$\frac{\partial}{\partial R} (q \rho w^*) - \frac{\partial}{\partial Z} (s \rho u^*) = \frac{g}{\theta_0} \frac{\partial Q}{\partial R}. \tag{3.20}$$

If we make use of (3.15) to define the streamfunction  $\psi^*$  by

$$(\rho u^*, \rho w^*) = \left( -\frac{\partial \psi^*}{\partial Z}, \frac{\partial R \psi^*}{R \partial R} \right), \tag{3.21}$$

we can write the transverse circulation equation (3.20) as

$$\frac{\partial}{\partial R} \left( q \frac{\partial R \psi^*}{R \partial R} \right) + \frac{\partial}{\partial Z} \left( s \frac{\partial \psi^*}{\partial Z} \right) = \frac{g}{\theta_0} \frac{\partial Q}{\partial R}, \tag{3.22a}$$

which is the analogue of (2.11a). The boundary conditions for (3.22a) are

$$\left. \begin{aligned} \psi^*(0, Z) &= \psi^*(R, Z_T) = 0 \\ R \psi^* &\rightarrow 0 \text{ as } R \rightarrow \infty \\ R \psi^*_\delta &= \frac{f}{\zeta_0} \rho_0 c_D |v_0| \frac{1}{2} (R^2 - r_0^2) \end{aligned} \right\}, \tag{3.22b}^3$$

the last of which can be derived from (2.8), (3.5), (3.9) and (3.21). In numerical calculation the condition  $R \psi^* \rightarrow 0$  as  $R \rightarrow \infty$  must be replaced by an approximate condition at finite  $R$ . This is discussed in the Appendix.

To summarize the transformed model we now collect the results (3.16), (3.14), (3.7), (3.19), (3.22), (3.21), (3.11) and (3.10) applied at  $Z = 0$ . These results are shown on the right side of Table 1. A single step in the numerical integration proceeds as follows. Knowing  $\theta(R, Z)$  and  $r_0(R)$  from an initial condition or a previous time step we solve (3.23) for  $r(R, Z)$ . After using (3.24)–(3.26) to determine  $q$  and  $s$  we solve (3.27) for  $\psi^*(R, Z)$ . After computing  $u^*$  and  $w^*$  from (3.28) we predict new values of  $\theta(R, Z)$  and  $r_0(R)$  from (3.29) and (3.30). Since  $r$  is one of the dependent variables the transformation of the results from potential radius  $R$  back to actual radius  $r$  is straightforward.

<sup>3</sup> Eqs. (3.23)–(3.30) are given in Table 1.

Comparing the right side of Table 1 with the left side we note several ways that the transformed model differs from the original model: the horizontal coordinate is  $R$  rather than  $r$ , which results in a stretching of positive relative vorticity regions and a shrinking of negative relative vorticity regions; the equation for  $\theta$  contains no  $u^*$  term, the equation for  $r$  contains no  $w^*$  term, and as a result the transverse circulation equation (3.27) contains no cross derivative terms;  $q$  plays the role of static stability and  $s$  the role of inertial stability. As long as we are dealing with stable vortices, we have  $q > 0$  and  $s > 0$ , in which case (3.27) is elliptic.

In passing we note that as an alternative to (3.30) it is possible to derive an integral condition on  $\partial r / \partial T$  by multiplying (3.10) by  $\rho$ , integrating over the depth of the free atmosphere, and using (3.15), (3.21), the boundary conditions  $w^* = 0$  at  $Z = Z_T$ ,  $Ru^* \rightarrow 0$  and  $R\psi_\delta^* \rightarrow 0$  as  $R \rightarrow \infty$  to obtain

$$\frac{\partial}{\partial T} \int_0^{Z_T} \frac{r^2}{2} \rho dZ = R\psi_\delta^*, \quad (3.31)$$

a statement that the mass within an absolute angular momentum surface is increasing with time if there is cyclonic flow at the top of the boundary layer ( $R > r_0$ ).

#### 4. Tropical cyclone structure in the potential radius coordinate

In order to gain a better understanding of the transformed model we now examine typical distributions

of  $v(r, z)$ ,  $v(R, Z)$ ,  $R(r, z)$ ,  $r(R, Z)$ ,  $\rho q(R, Z)$ ,  $\rho s(R, Z)$  and  $[q(R, Z)/s(R, Z)]^{1/2}$ . We first examine observational data composited by William Gray's tropical cyclone research group at Colorado State University. In particular, we use an analytical fit to the large typhoon composite tangential winds of Merrill (1982). The large typhoon composite is made up of all tropical cyclones in the northwest Pacific in which the central pressure was less than 980 mb and the average radial distance to the outermost closed isobar exceeded  $6^\circ$  latitude. These large systems comprise 36% of all typhoons in the northwest Pacific.

The calculation of potential vorticity requires knowledge of  $\theta$  in addition to knowledge of  $v$ . We have obtained  $\theta$  from  $v$  by solving the thermal wind equation (2.12) radially inward, starting from a standard atmosphere profile of  $\theta$  at  $r = 1500$  km. The standard atmosphere profile which was used is a slightly smoothed version of the mean tropical clear area sounding of Gray *et al.* (1975). The corresponding profile of  $N^2 = (g/\theta_0)(\partial\theta/\partial z)$  is shown in Fig. 1. For reference the profile of  $\rho/\rho_0$  is also shown.

Isopleths of  $v(r, z)$  and  $v(R, Z)$  for the large typhoon composite are shown in Fig. 2. In  $(r, z)$  space the radius of maximum wind is  $\sim 100$  km while in  $(R, Z)$  space it is  $\sim 375$  km. In general,  $(R, Z)$  space provides stretching when  $v > 0$  and shrinking when  $v < 0$ . In Fig. 3 we show the fields of  $R(r, z)$  and  $r(R, Z)$ . Since the  $R$  surfaces are also absolute angular momentum surfaces one possible interpretation is that the transverse circulation has swept high absolute

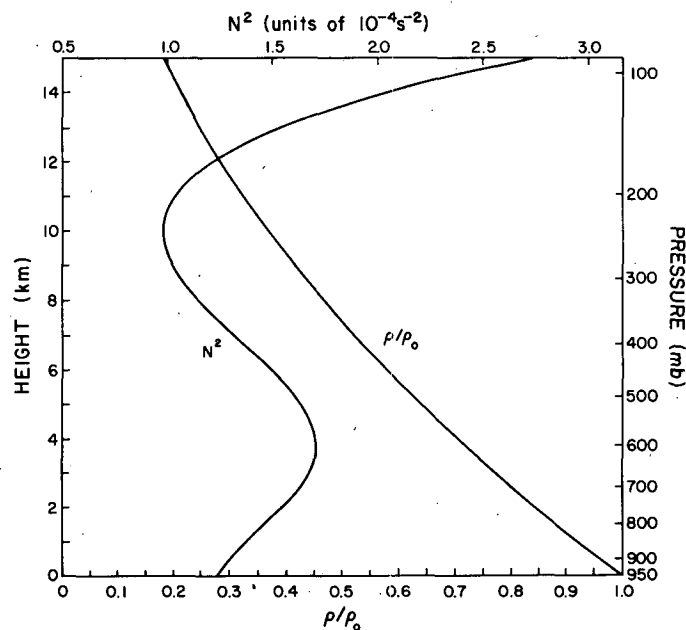


FIG. 1. The curve  $\rho/\rho_0 = [1 - (gz/c_p\theta_0)]^{(1-\kappa)/\kappa}$  gives the vertical variation of the pseudodensity. The curve  $N^2 = (g/\theta_0)(\partial\theta/\partial Z)$  gives the vertical variation of the static stability computed from the mean tropical clear area temperature profile of Gray *et al.* (1975).

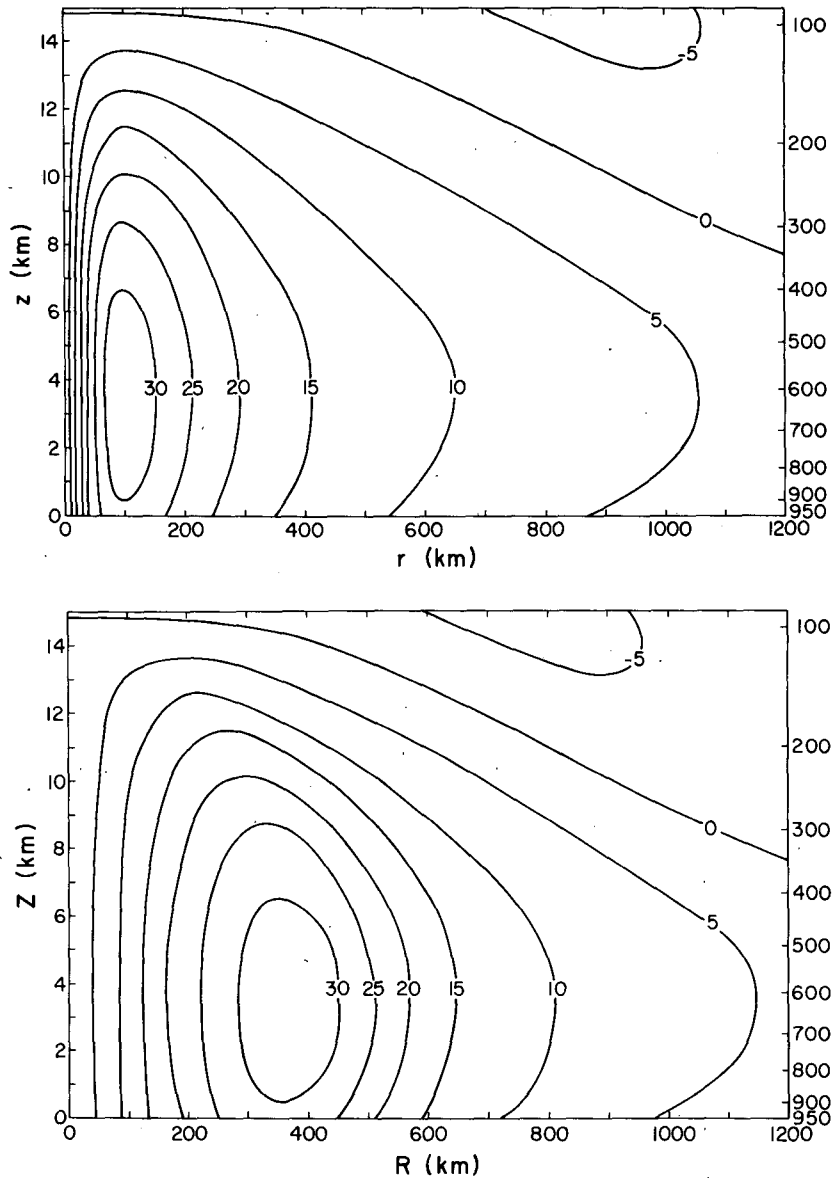


FIG. 2. Isopleths of tangential wind  $v$  ( $m s^{-1}$ ) in  $r, z$  space (top) and  $R, Z$  space (bottom). Note how the potential radius coordinate stretches the region of large cyclonic vorticity.

angular momentum in at low levels and low absolute angular momentum out at high levels. Along the dotted lines in Fig. 3 the tangential wind vanishes and hence  $R = r$ .

According to (3.27) the transverse circulation is determined by the forcing  $Q$  and the vortex structure functions  $q$  and  $s$ . The fields of  $\rho q(R, Z)$  and  $\rho s(R, Z)$  are shown in Fig. 4. The variation of  $\rho q$  is more than a factor of 50 while that of  $\rho s$  is more than a factor of 500. It is the inner core region which has both high “static” and “inertial” stability. In the next section we shall show that the generalized Rossby radius, which is proportional to  $(q/s^{1/2})$ , is a measure

of the rotational constraint on the cyclone and plays an important role in development. The field of  $(q/s^{1/2})$  is shown in Fig. 5. Below 200 mb and inside 600 km the relatively smaller Rossby radii signify a stronger rotational constraint and a relative tendency for adjustment of wind to pressure (e.g., Schubert *et al.*, 1980) As we shall show in the next section, the terms “strong rotational constraint” and “adjustment of wind to pressure” are synonymous with “efficient heating.”

The rawinsonde composite data set used to construct Figs. 2–5 does not resolve the inner core region of the cyclone. In order to better understand this inner

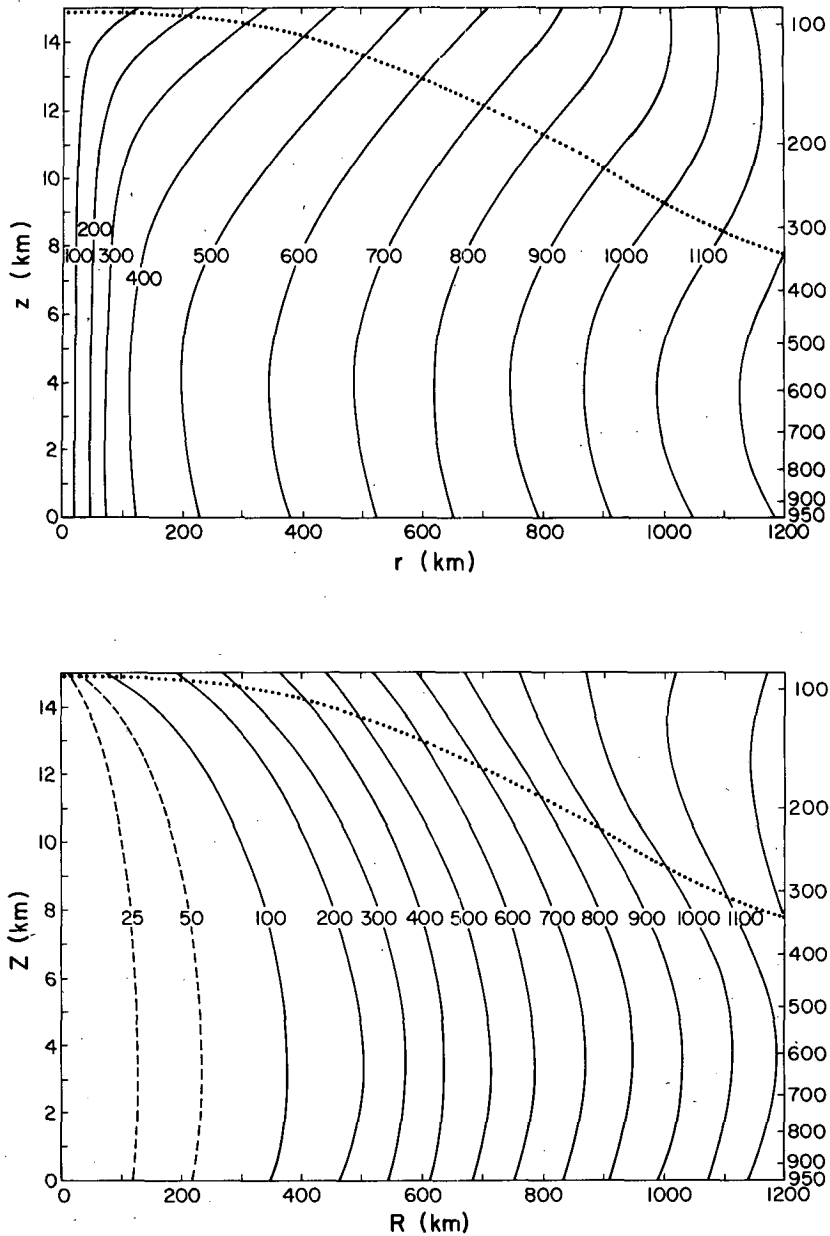


FIG. 3. Isopleths of  $R$  (km) in  $r, z$  space (top) and  $r$  (km) in  $R, Z$  space (bottom). Along the dotted lines the tangential wind vanishes so that  $R = r$ .

region we present in Fig. 6 isopleths of  $v(r, z)$  and  $R(r, z)$  based on aircraft data collected at five levels in hurricane Hilda [see Hawkins and Rubsam (1968) for an extensive discussion of this hurricane]. We note that the maximum tangential wind ( $\sim 45 \text{ m s}^{-1}$ ) lies at a radius of  $\sim 25 \text{ km}$ , through which runs the 200 km potential radius surface. Thus, for this case, the use of  $R$  as a coordinate results in an eightfold stretching of the lower tropospheric inner core region. Inner region values of the generalized Rossby radius are approximately one-tenth of the values at large radius.

##### 5. The generalized Rossby radius and the distribution of local temperature change

In order to understand how  $q$  and  $s$  influence the balance of terms in the thermodynamic equation (3.11), we consider an inviscid situation where  $q$  and  $s$  are constants and  $Q(R, Z)$  is given by

$$Q(R, Z) = \begin{cases} \hat{Q} \sin\left(\frac{\pi Z}{Z_T}\right), & R < \hat{R}, \\ 0, & R > \hat{R}, \end{cases} \quad (5.1)$$



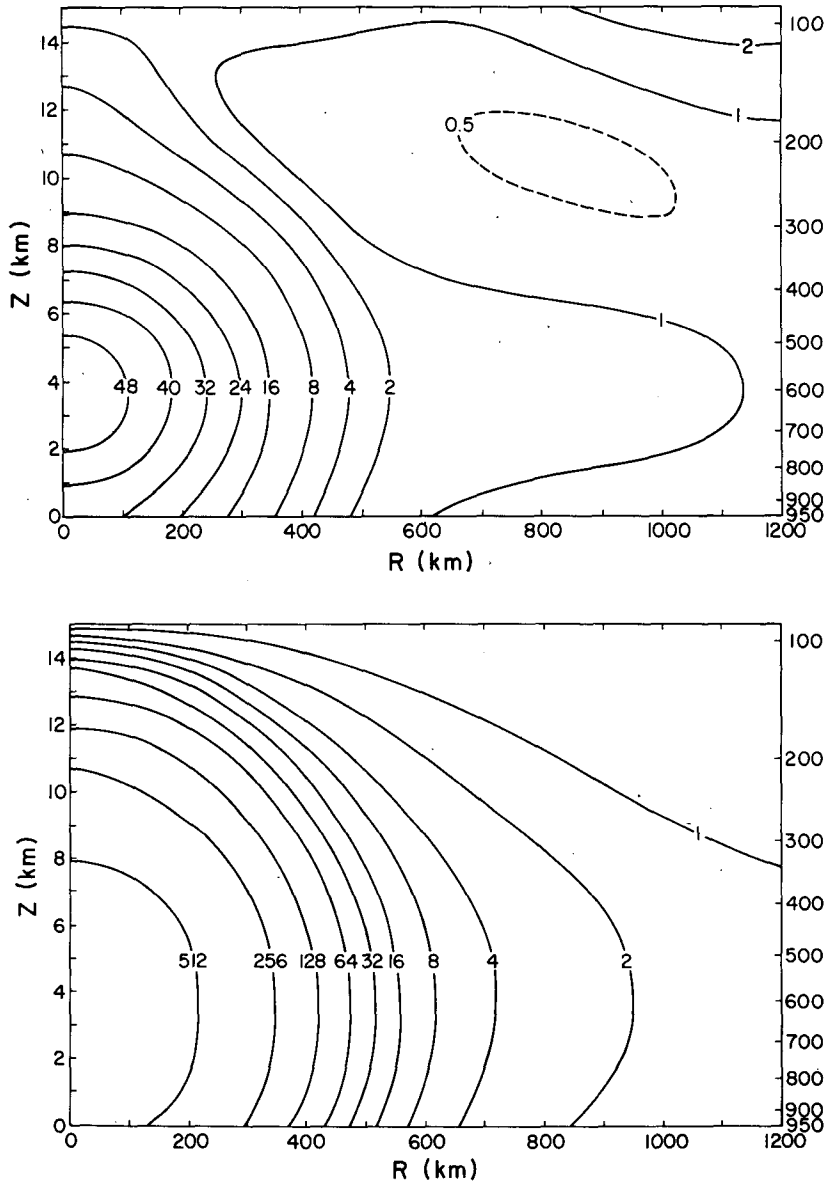


FIG. 4. Isopleths of  $\rho q$  (top) in units of  $N^2$  [where  $N^2 = (1.2 \cdot 10^{-2} \text{ s}^{-1})^2$  is the vertically averaged value of  $(g/\theta_0)(\partial\theta/\partial Z)$  at large radius] and  $\rho s$  (bottom) in units of  $f^2 = (5 \times 10^{-5} \text{ s}^{-1})^2$ .

where the parameters  $\hat{Q}$  and  $\hat{R}$  give the magnitude and the horizontal scale of the heating. Using (5.1) in (3.27) and assuming  $\psi^*(R, Z) = \Psi^*(R) \sin(\pi Z/Z_T)$  we obtain

$$R \frac{d}{dR} \left( R \frac{d\Psi^*}{dR} \right) - (\mu^2 R^2 + 1)\Psi^* = 0, \quad (5.2a)$$

where  $\mu^{-1} = (q/s)^{1/2} Z_T/\pi$  is the generalized Rossby radius. Eq. (5.2a) holds in the regions  $0 \leq R < \hat{R}$  and  $\hat{R} < R < \infty$ . Across  $R = \hat{R}$  the streamfunction is continuous so that

$$[\Psi^*]_{\hat{R}^-}^{\hat{R}^+} = 0, \quad (5.2b)$$

while the radial derivative of the streamfunction jumps in such a way that

$$\left[ \frac{dR\Psi^*}{RdR} \right]_{\hat{R}^-}^{\hat{R}^+} = -\frac{g\hat{Q}}{\theta_0 q}. \quad (5.2c)$$

The solution of (5.2a) consists of linear combinations of the modified Bessel functions  $I_1(\mu R)$  and  $K_1(\mu R)$  in each region. However, the boundary conditions for  $R = 0$  and  $R \rightarrow \infty$  require that we discard  $K_1$  in the inner region and  $I_1$  in the outer region. Then, after determining the remaining two constants via (5.2b) and (5.2c), we obtain

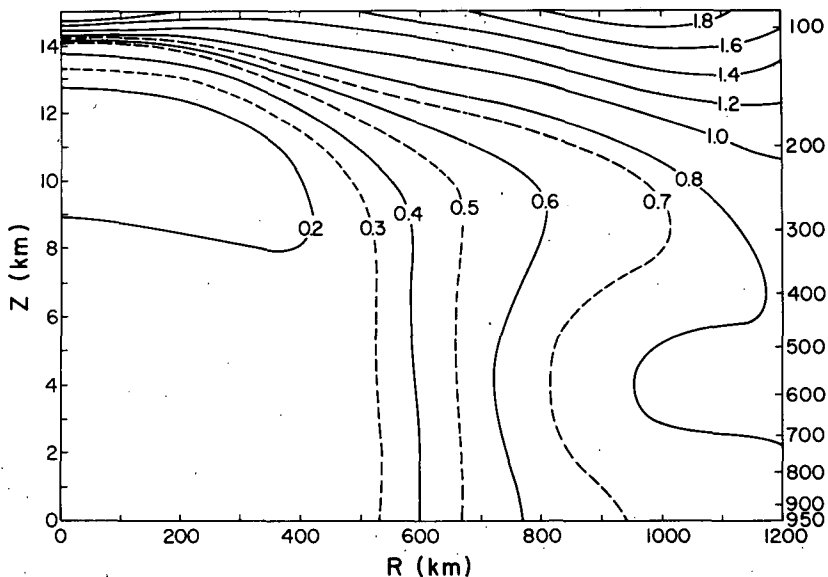


FIG. 5. Isopleths of the local Rossby radius  $(q/s)^{1/2}Z_T/\pi$  in units of  $(\bar{N}/f)(Z_T/\pi) \approx 1150$  km, which is the vertically averaged value of the Rossby radius at large distances from the origin.

$$\Psi^*(R) = \frac{g\hat{Q}}{\theta_0 q} \begin{cases} \hat{R}K_1(\mu\hat{R})I_1(\mu R), & R \leq \hat{R} \\ \hat{R}I_1(\mu\hat{R})K_1(\mu R), & R \geq \hat{R} \end{cases} \quad (5.3)$$

If we apply (3.11) at  $Z = Z_T/2$ , integrate over the heated area, and make use of (3.21), we obtain

$$\int_0^{\hat{R}} \frac{\partial \theta}{\partial T} R dR = \int_0^{\hat{R}} QR dR - \frac{\theta_0}{g} q \hat{R} \Psi^*(\hat{R}).$$

Then, using (5.3) and the fact that  $\int_0^{\hat{R}} QR dR = \hat{Q} \times \hat{R}^2/2$  when  $Z = Z_T/2$ , we obtain

$$\frac{\int_0^{\hat{R}} \frac{\partial \theta}{\partial T} R dR}{\int_0^{\hat{R}} QR dR} = 1 - 2I_1(\mu\hat{R})K_1(\mu\hat{R}), \quad (5.4)$$

which is a somewhat simplified (and transformed) version of Eq. (3.1) of Schubert and Hack (1982). A plot of this "efficiency" as a function of  $\mu\hat{R}$  is given in Fig. 7. The efficiency increases as  $\mu\hat{R}$  increases. Since

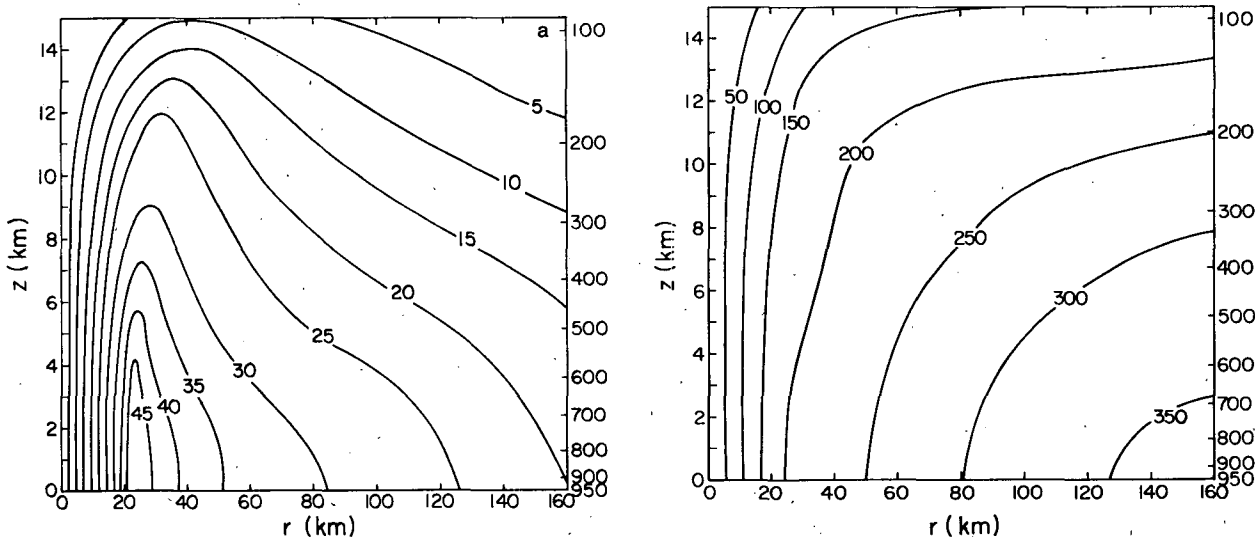


FIG. 6. Isopleths of (a) tangential wind  $v(r, z)$  in  $m s^{-1}$  and (b)  $R(r, z)$  in km for the inner region of Hurricane Hilda (see Hawkins and Rubsam, 1968).

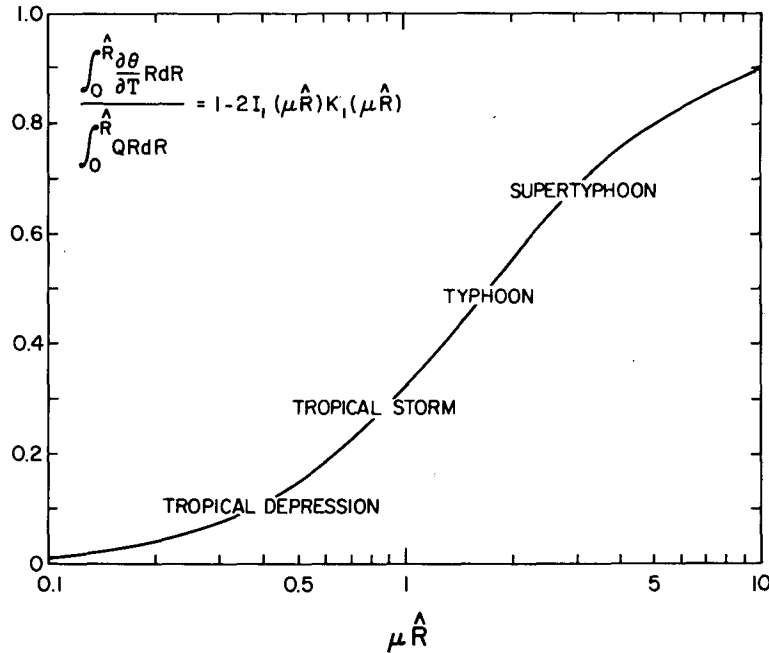


FIG. 7. A plot of the right hand side of (5.4) as a function of  $\mu \hat{R}$ .

$$\mu = \frac{f\pi}{NZ_T} \left( \frac{f + \frac{2v}{r}}{f\zeta} \right)^{1/2}$$

$\mu$  grows approximately as the square root of the absolute circulation. If the horizontal scale of the heating remains approximately constant in physical space,  $\hat{R}$  also grows as the square root of the absolute circulation since

$$R = \left( \frac{f + \frac{2v}{r}}{f} \right)^{1/2} r.$$

Thus, when viewed in the potential radius coordinate there are two effects which can lead to increased efficiency—the shrinkage of the generalized Rossby radius (i.e., increased  $\mu$ ) and the growth in the dynamic size of the heated region (i.e., increased  $\hat{R}$ ). Sometimes in tropical cyclone development the angular momentum surfaces and the “edge” of the highly convective region both move inward in physical space. As long as the angular momentum surfaces move inward faster than the edge of the convective region, the dynamic size of the heated region increases.

Although  $\mu$  can vary significantly in the convective region of a tropical cyclone, it is possible to compute convective region averages of  $\mu$  for various stages of development. This has been done by G. Holland (personal communication, 1982) using northwest Pacific composite data sets for different development stages. Roughly speaking, Holland’s results give rise

to the labeling shown in Fig. 7, i.e., a steady climb up the efficiency curve. Thus, the view presented here is that tropical cyclone development is essentially a nonlinear process<sup>4</sup> in which an approximately fixed amount of total latent heat release leads to increasing  $\mu \hat{R}$  and increasing local temperature change.

### 6. Concluding remarks

Using potential radius  $R$  as the horizontal coordinate and introducing the new components ( $u^*$ ,  $w^*$ ) of the divergent flow we have transformed and simplified the Eliassen balanced vortex model. Although the transformed model has certain similarities with the two-dimensional semi-geostrophic equations used in frontogenesis studies, further analytical progress with it appears to be more difficult. In frontogenesis studies, one can assume potential vorticity is conserved so that an initial uniform potential vorticity field will remain so. Then considerable understanding of surface fronts can be obtained with the uniform potential vorticity model or even the zero potential vorticity model, while upper level fronts can be studied with the discontinuous potential vorticity model (Hoskins and Bretherton, 1972). In contrast, the tropical cyclone problem forces us to cope with sources of potential vorticity and with large variations in both  $q$  and  $s$  (which has a simpler form in semi-geostrophic theory).

<sup>4</sup> For a related discussion of the role of nonlinear processes in tropical storm development the reader is referred to the paper of Ooyama (1982).

If numerical methods are to be used, does the transformed model have any advantage over the original Eliassen model? First of all there is the advantage of being able to easily display the results in both  $(R, Z)$  and  $(r, z)$  space and to view the transverse circulation as  $(u, w)$  and  $(u^*, w^*)$ . Second, the transformed model can be solved with fewer degrees of freedom in the horizontal direction because the inner core region is automatically stretched.

In the past a variety of methods have been used to solve equations of the form (2.16) or (3.27), e.g., successive over-relaxation, alternating direction implicit, and direct methods. Recently, much more effective multigrid methods (Brandt, 1977) have become available. We are presently investigating the use of multi-grid and spectral methods for the solution of (3.23)–(3.30).

*Acknowledgments.* The authors are grateful to Scott Fulton, Mark DeMaria, Gerald Taylor, Greg Holland, Duane Stevens and William Gray for their valuable comments and to Paul Ciesielski for his help with the calculations. We are also indebted to Odilia Panella for her help in preparing the manuscript. This research was supported by NSF Grants ATM-8009799 and ATM-8207563.

#### APPENDIX

##### Boundary Condition for Eq. (3.21)

When the transverse circulation equation (3.21) is solved numerically the boundary condition  $R\psi^* \rightarrow 0$  as  $R \rightarrow \infty$  must be replaced by an approximate condition at large but finite  $R$ . To derive an approximate condition we follow the general argument developed by Hack and Schubert (1981) for primitive equation models. Suppose that at some large  $R$  the vortex is very weak and the heating is negligible so that  $r \approx R$ ,  $\zeta \approx f$ ,  $\rho q \approx (g/\theta_0)(\partial\theta/\partial Z) = N^2(Z)$  and  $Q \approx 0$ . Then (3.21) becomes

$$\frac{1}{f^2} \frac{\partial}{\partial R} \left( \frac{\partial R \psi^*}{R \partial R} \right) + \frac{\rho}{N^2} \frac{\partial}{\partial Z} \left( \frac{\partial \psi^*}{\rho \partial Z} \right) = 0, \quad (\text{A1})$$

for large  $R$ . We now define the vertical finite Sturm-Liouville transform pair by

$$\Psi_n^*(R) = \int_0^{Z_T} \psi^*(R, Z) Z_n(Z) \frac{N^2(Z)}{\rho(Z)} dZ, \quad (\text{A2})$$

$$\psi^*(R, Z) = \sum_n \Psi_n^*(R) Z_n(Z), \quad (\text{A3})$$

where  $Z_n(Z)$  is the yet-to-be-determined kernel of the transform.

If we apply the vertical transform (A2) to (A1), integrate by parts twice, use the upper and lower boundary conditions  $\psi^* = 0$  at  $Z = 0, Z_T$ , and require that the kernel  $Z_n(Z)$  satisfy the Sturm-Liouville problem

$$\left. \begin{aligned} \rho \frac{\partial}{\partial Z} \left( \frac{\partial Z_n}{\rho \partial Z} \right) + \frac{N^2}{c_n^2} Z_n &= 0 \\ Z_n &= 0 \quad \text{at } Z = 0, Z_T \end{aligned} \right\}, \quad (\text{A4})$$

we obtain

$$R^2 \frac{d^2 \Psi_n^*}{dR^2} + R \frac{d \Psi_n^*}{dR} - (\mu_n^2 R^2 + 1) \Psi_n^* = 0, \quad (\text{A5})$$

where  $\mu_n = f/c_n$ . If we discard the modified Bessel function solution which grows in  $R$ , the solution of (A5) can be expressed as a constant times the first-order modified Bessel function  $K_1(\mu_n R)$ . Since

$$\frac{d}{RdR} \{RK_1(\mu_n R)\} = -\mu_n K_0(\mu_n R)$$

the function of  $\Psi_n^*(R)$  obeys

$$K_1(\mu_n R) \frac{dR \Psi_n^*(R)}{RdR} + \mu_n K_0(\mu_n R) \Psi_n^*(R) = 0, \quad (\text{A6})$$

for large  $R$ . If we apply (A6) at some large radius  $\hat{R}$  and if we then take the inverse transform (A3), we obtain

$$\frac{dR \psi^*}{dR} + \sum_n \frac{\mu_n R K_0(\mu_n R)}{K_1(\mu_n R)} \Psi_n^*(R) Z_n(Z) = 0$$

at  $R = \hat{R}. \quad (\text{A7})$

Since  $\Psi_n^*$  is determined from (A2), the condition (A7) relates the boundary value of the radial derivative of  $\psi^*$  at a particular level to the boundary values of  $\psi^*$  at all other levels.

#### REFERENCES

- Brandt, A., 1977: Multi-level adaptive solutions to boundary-value problems. *Math. Comput.*, **31**, 333–390.
- Charney, J. G., and A. Eliassen, 1964: On the growth of the hurricane depression. *J. Atmos. Sci.*, **21**, 68–75.
- Eliassen, A., 1952: Slow thermally or frictionally controlled meridional circulation in a circular vortex. *Astrophys. Norv.*, **5**, 60 pp.
- , 1962: On the vertical circulation in frontal zones. *Geophys. Publ.*, **24**, 147–160.
- Gill, A. E., 1981: Homogeneous intrusions in a rotating stratified fluid. *J. Fluid. Mech.*, **103**, 275–295.
- Gray, W. M., E. Ruprecht and R. Phelps, 1975: Relative humidity in tropical weather systems. *Mon. Wea. Rev.*, **103**, 685–690.
- Hack, J. J., and W. H. Schubert, 1981: Lateral boundary conditions for tropical cyclone models. *Mon. Wea. Rev.*, **109**, 1404–1420.
- Hawkins, H. F., and D. T. Rubsam, 1968: Hurricane Hilda, 1964. II: Structure and budgets of the hurricane on 1 October 1964. *Mon. Wea. Rev.*, **96**, 617–636.
- Hoskins, B. J., 1975: The geostrophic momentum approximation and the semi-geostrophic equations. *J. Atmos. Sci.*, **32**, 233–242.
- , and F. P. Bretherton, 1972: Atmospheric frontogenesis models: mathematical formulation and solution. *J. Atmos. Sci.*, **29**, 11–37.
- , and I. Draghici, 1977: The forcing of ageostrophic motion according to the semi-geostrophic equations and in an isentropic coordinate model. *J. Atmos. Sci.*, **34**, 1859–1867.

- McWilliams, J. C., and P. R. Gent, 1980: Intermediate models of planetary circulations in the atmosphere and ocean. *J. Atmos. Sci.*, **37**, 1657-1678.
- Merrill, R. T., 1982: A comparison of large and small tropical cyclones. Atmos. Sci. Pap. No. 252, Colorado State University, Fort Collins, 75 pp.
- Ogura, Y., 1964: Frictionally controlled, thermally driven circulations in a circular vortex with application to tropical cyclones. *J. Atmos. Sci.*, **21**, 610-621.
- Ooyama, K., 1964: A dynamical model for the study of tropical cyclone development. *Geofis. Int.*, **4**, 187-198.
- , 1969a: Numerical simulation of the life cycle of tropical cyclones. *J. Atmos. Sci.*, **26**, 3-40.
- , 1969b: Numerical simulation of tropical cyclones with an axisymmetric model. *Proc. WMO/IUGG Symp. on Numerical Weather Prediction*, Tokyo, 1968, III:81-88.
- , 1982: Conceptual evolution of the theory and modeling of the tropical cyclone. *J. Meteor. Soc. Japan*, **60**, 369-379.
- Peng, Li, and H. L. Kuo, 1975: A numerical simulation of the development of tropical cyclones. *Tellus*, **27**, 133-144.
- Schubert, W. H., and J. J. Hack, 1982: Inertial stability and tropical cyclone development. *J. Atmos. Sci.*, **39**, 1687-1697.
- , ———, P. L. Silva Dias and S. R. Fulton, 1980: Geostrophic adjustment in an axisymmetric vortex. *J. Atmos. Sci.*, **37**, 1464-1484.
- Shapiro, L. J., and H. E. Willoughby, 1982: The response of balanced hurricanes to local sources of heat and momentum. *J. Atmos. Sci.*, **39**, 378-394.
- Shutts, G. J., 1980: Angular momentum coordinates and their use in zonal, geostrophic motion in a hemisphere. *J. Atmos. Sci.*, **37**, 1126-1132.
- , and A. J. Thorpe, 1978: Some aspects of vortices in rotating, stratified fluids. *Pure Appl. Geophys.*, **116**, 993-1006.
- Sundqvist, H., 1970: Numerical simulation of the development of tropical cyclones with a ten-level model. Part I. *Tellus*, **22**, 359-390.
- Willoughby, H. E., J. Clos and M. Shoreibah, 1982: Concentric eye walls, secondary wind maxima and the evolution of symmetric hurricane vortices. *J. Atmos. Sci.*, **39**, 395-411.